

Scanned Monocular Sonar and the Doorway Problem

Lindsay Kleeman

Department of Electrical and Computer Systems Engineering
Monash University, Australia

Abstract

A sonar system is presented that relies on scanning a single ultrasonic transducer and measuring echo amplitude and arrival times. Bearing angles to targets are estimated far more accurately than the transducer beamwidth as obtained with conventional sonar rings based on the Polaroid ranging module. A Gaussian beam characteristic is fitted using least squares to the amplitudes of corresponding echoes in the scan to obtain an estimate of the bearing to specular targets. As an illustration of the information gain over conventional sonar rings, the sensor approach is used on a mobile robot to find, traverse and map doorways reliably and with minimal algorithmic effort. This is compared with other work that claims the problem is difficult to solve using a conventional sonar ring of 24 Polaroid ranging modules [4].

1. Introduction

Sonar or ultrasonic sensing is often deployed on mobile robots for ranging to objects in unknown environments [2, 3, 4, 6, 10, 12, 13, 14, 15]. A ring of sonar ranging modules is commonly employed and range to the nearest target is captured from each transducer acting in isolation. The important issue of bearing accuracy is neglected in sonar rings. Bearing to ultrasonic targets is *roughly* estimated to within the beamwidth of the transducer by examining the transducer pointing direction only. Grid based mapping schemes [6] attempt to alleviate the problem by probabilistically combining hopefully independent views of common features to accumulate votes on the presence of targets. To provide more accurate bearing estimation and even target classification, multiple coordinated transducer sonar systems have been developed [8, 9, 14, 16]. These rely on associating ultrasonic echoes from multiple receivers [14, 16] and multiple transmitters [8, 9]. The signal processing and data capture hardware is necessarily more complex and expensive than sonar rings.

This paper presents an intermediate approach that relies on rapidly scanning a single transducer and collecting range *and amplitude* information for all echoes. Bearing to targets can be robustly estimated based on a least squares fit to a known beam pattern characteristic. The approach is straightforward in hardware and signal

processing, yet achieves good bearing accuracies to multiple simultaneous targets in the field of insonification. Work by Bozma and Kuc [1, 2] uses scanned sonar sensing for mapping rough surfaces based on energy, duration and range maps. This paper concentrates on specular environments found commonly indoors and uses a new bearing estimation approach. The work presented here also has application to an advanced multiple transducer system [8, 9] as a high speed “scout” to quickly locate targets for relatively slower classification later by the multiple transducer system.

A good mobile robot demonstration of scanned monocular sonar approach is the doorway finding and traversal problem. This same problem is considered difficult using conventional sonar ring sensing [4] and requires large amounts of high level “domain specific knowledge” to achieve a 78% success rate solution. The difficulty lies in three areas:

1. Inaccurate bearing information makes location of door openings difficult;
2. The effectively low scan angle resolution of a sonar ring (eg 15 degrees in [4]) makes the reliable detection of edge targets almost impossible due to their low returned energy [10]; and
3. Nearer targets mask further targets using first return triggered sonar systems. For example, a nearby wall can obscure the approaching doorway.

The scanned monocular sonar system presented here overcomes all three of these difficulties by low level sensor data processing based on physical models of the specular reflectors and the transducer beam pattern. The high level algorithm for doorway finding and traversal then becomes relatively straightforward.

The paper is structured from the “bottom up” as follows. In section 2, the basic hardware is described for implementing the scanned sonar. Low level signal processing is presented for the extraction of echo data, such as arrival time and amplitude. Association of echoes between different scan angles is addressed in section 4, and section 5 describes the least squares Gaussian fit of beam pattern to determine the bearing estimate. Section 5 presents some results to characterise the sensor accuracy and section 6 describes the door finding and traversal algorithm. Results of doorway trials are given in section 7.

Conclusions and future extensions are outlined in the last section.

2. Sonar Hardware

A Polaroid 7000 Series electrostatic transducer is interfaced to a single board computer via custom designed transmit and receiving electronics as shown in Figure 1. Transmitting is performed by a 10 microsecond 0 V pulse on a 300 V biased transducer. This produces a short acoustic pulse of the order of 80 microseconds duration. Several such pulses are shown in Figure 2. The receiver circuitry has sufficient signal to noise ratio to receive echoes from plane targets out to approximately 8 metres range. The full echo waveform is captured via a 12 bit ADC sampling at 1 Mhz at a constant gain. This prototype sampling rate can be reduced considerably in a mass produced system when only echo amplitude and arrival time are of interest, as is the case in the scanned monocular sonar presented here. A geared DC servo motor is used to control the panning angle and/or speed of rotation. The angle of output shaft of the gearbox connected to the transducer is feedback to a PID motion control card using an optical encoder with resolution of 0.18 degrees. The number scan angles per revolution can varied up to 2000, although 80 to 200 is used in practice.

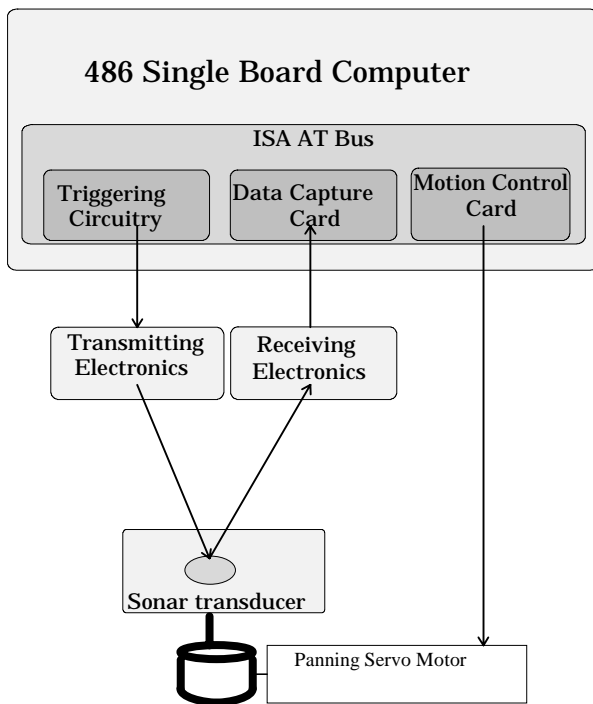


Figure 1 - Scanned sonar hardware configuration.

[59 -41]	[218 -147]	[1198 -925]	[61 -47]
E 46748	E 379940	E 10409113	E 36457
EW 47	EW 19	EW 28	EW 44
MW 16	MW 8	MW 12	MW 13
AT 3860.6	AT 4331.1	AT 4582.0	AT 9188.1
CW 16.6	CW 8.0	CW 6.6	CW 6.8

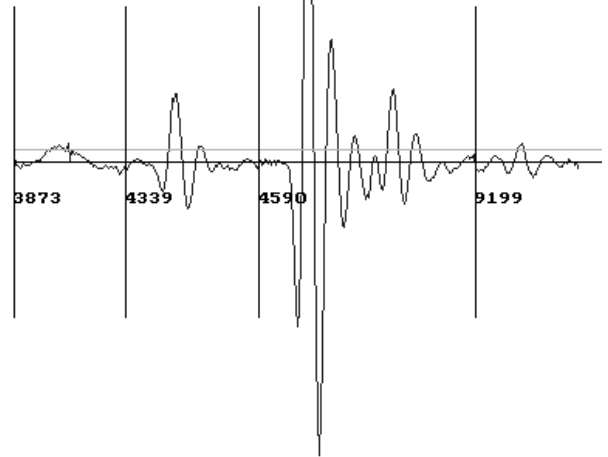


Figure 2 - A set of four echo groups from the one transmitted pulse with intervening time removed. The sample number in microseconds is shown at the beginning of each echo

3. Low Level Signal Processing

The complete received signal is processed to extract individual echoes and determine their arrival time and amplitude. Echoes are identified by the two successive samples exceeding a threshold of 7 standard deviations of noise above the mean of the noise present on the receiver channel when no pulse is transmitted. A fixed number of samples are retained before the threshold is first exceeded and after the signal drops below the threshold so that a complete echo pulse is captured and the oscillation of the pulse cannot cause multiple registration of the one echo. When echoes overlap, it is unavoidable that multiple echoes are treated as one, as occurs in the third group in Figure 2. The bearing estimation process described below addresses this problem.

Each echo is processed to determine the maximum minus minimum which is henceforth called the echo *amplitude*. The arrival time can be optimally estimated using a matched filter as described in [8], however such accuracy and the accompanying computation burden are not required here, since differences in arrival times are not required as in [8]. It is sufficient and faster to use the time the signal crosses two thresholds, called the left and right thresholds as shown in Figure 3. The left

threshold is defined as the average of the pulse maximum and the first minimum to the left of that maximum. The right threshold is defined similarly. The average of these two crossing times, denoted by T_l and T_r in Figure 3, minus an offset is used as the arrival time. This simple algorithm can lead to moderate errors when the signal to noise ratio is poor in the case of weak echoes.

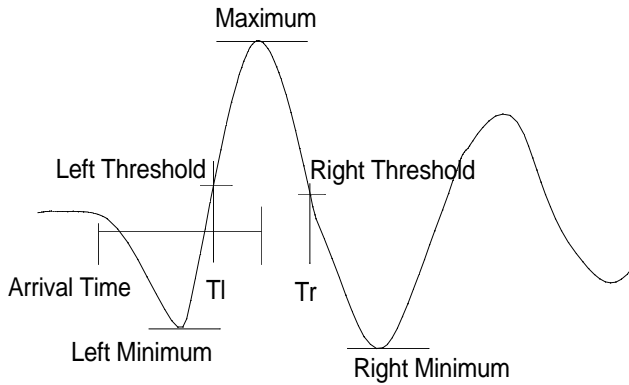


Figure 3 - Arrival Time Estimation

4. Associating Echoes between Scan Angles

In order to perform bearing estimation, echoes that arise from the same physical source insonified at different scan angles need to be associated with one another. Due to the possibility of closely spaced targets in range, this is a non-trivial problem in practice. Incorrect association can lead to large errors in bearing estimation and also in phantom targets being generated. For example, a smooth close target can generate discernible echoes over a range of 50 degrees and if both extreme ends of the data are not associated to the centre without breaks, phantom targets could be perceived to be large angles from their real physical source. This situation could also be prevented at higher levels (at a greater cost in robustness and processing time!)

The association is performed using both the amplitude and arrival time as follows: A seed echo is found from maximum amplitude echo not already part of an association. Associates are obtained by searching successive scan angles in both directions away from the seed by looking for echoes with an amplitude within a certain ratio of the previous associate. Of these echoes, the nearest arrival time to the previous associate is chosen provided it is not further away than a bound. Up to one scan angle is allowed to be skipped before no more associates are included.

5. Target Bearing Estimation

Several parameters of echoes have been investigated for use in bearing estimation. For example echo energy and duration have been proposed by Bozma and Kuc [2] as useful characteristics. Other features considered include second order moment (MW), zero crossing width around the maximum (CW) and echo width that contains “most” of the total energy (EW) - refer to Figure 2 for examples of the use of (acronyms). The difficulty with these measures in practice is that noise and overlapping echoes affect the range over which the echo is defined. Where does an echo start and end in the presence of noise and other echoes? The amplitude of the echo has been found to be a robust and simple parameter to estimate bearing. An attractive, but more complex, alternative is to use the identity of the best template match of a set of echo templates generated *a priori* for different angles [8].

In normal air flow conditions of an air conditioned building, the amplitude of echoes from the same reflector at the same angle to the transducer varies significantly with time, whilst still maintaining the same pulse shape. As an illustration, 30 echo amplitudes were measured at one degree intervals from a plane and an edge. Figure 4 displays the standard deviation of the amplitude as a function of mean amplitude. The spread of the results is most likely due to the varying air turbulence and temperature mix of the air throughout the experiments. Nevertheless the standard deviation tends to be proportional to the echo amplitude for different angles observing the same target through the same air column. A physical explanation of this process is that the air turbulence fluctuates the echo amplitude and the beam pattern attenuates the incident pressure wave.

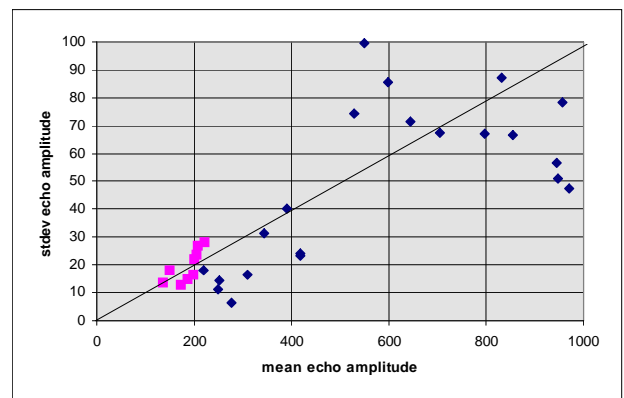


Figure 4 - Amplitude fluctuation versus amplitude for a plane and lower amplitude edge.

Kuc and Viard [11] have shown that the beam pattern, $p(\theta)$, for a circular transducer is approximately Gaussian. Multiplicative noise N , has been imposed on the Gaussian beamwidth in this paper to model air turbulence and temperature mixing effects:

$$p(\theta) = p_{\max} \exp^{-2\left(\frac{\theta-\alpha}{\theta_0}\right)^2} N \quad (1)$$

where θ_0 is half-angle of the beam width of the transducer, and α is the bearing to the target. Taking the log of both sides

$$\log(p(\theta)) = \log(p_{\max}) - 2\left(\frac{\theta-\alpha}{\theta_0}\right)^2 + \log(N) \quad (2)$$

The log of amplitude is now a quadratic in scan angle, θ and moreover the noise becomes additive noise. Assuming that N is statistically independently of θ , a least squares estimate of the quadratic is chosen. The maximum 7 amplitudes with consecutive scan angles are used. Given a column vectors of log echo amplitudes $\mathbf{P}=[\log(p_1).. \log(p_n)]^T$ and corresponding scan angles $[\theta_1.. \theta_n]^T$ the matrix \mathbf{M} is defined as

$$\mathbf{M} \equiv \begin{bmatrix} 1 & \theta_1 & \theta_1^2 \\ .. & .. & .. \\ 1 & \theta_n & \theta_n^2 \end{bmatrix} \quad (3)$$

A least square solution for the quadratic coefficients a , b and c is obtained for the following problem

$$\mathbf{P} = \mathbf{M} \begin{bmatrix} c \\ b \\ a \end{bmatrix} \quad (4)$$

from the pseudo-inverse of the rectangular matrix \mathbf{M} as follows:

$$\begin{bmatrix} c \\ b \\ a \end{bmatrix} = (\mathbf{M}^T \mathbf{M})^{-1} \mathbf{M}^T \mathbf{P} \quad (5)$$

The bearing, half angle beamwidth and maximum amplitude are now given by

$$\begin{aligned} \theta_0 &= \sqrt{\frac{-2}{a}} \\ \alpha &= \theta_0 b / 2 \\ p_{\max} &= \exp(c + 2\alpha^2) \end{aligned} \quad (6)$$

By examining the estimated beamwidth against measured beamwidth characteristics of the transducer¹, spurious bearing estimates can be rejected in cases where overlapping echoes are received or incorrect associations are made. An example set of amplitude and range measurements are shown in Figure 5, along with the extracted bearing angles to targets. The amplitude of an echo is display in Figure 5 as a light grey line at an angle of 30 degrees to the radial line from the robot position of range length and at the scan angle. The bearing estimates and associate amplitude estimates are shown as dark lines.

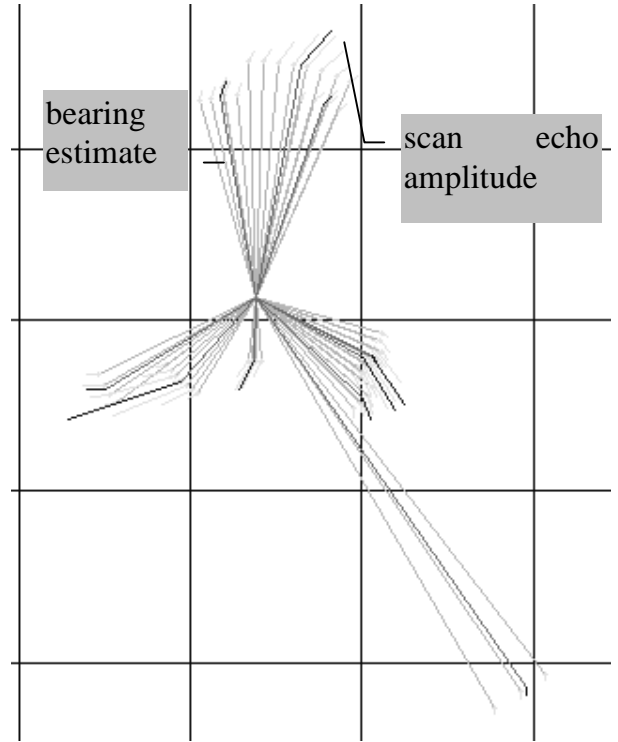


Figure 5 - Example of scanned amplitudes against scan angle and the estimated bearings (darker).

¹ Because the spectrum of the pulse is broad (~20 kHz) and also varies with range and absorption properties of air (dependent on temperature and humidity) there is no clearly defined wavelength. This means that the beamwidth of the transducer depends on range and ambient conditions.

6. Sensor Performance

The standard deviation of the 30 samples of range and bearing to a plane positioned at 0 degrees bearing was measured over a 4 metre range and summarised in Figure 6. The means of both range and bearing agreed within measurement error which suggests that the sensor has little measurement bias. The results compare well with multiple transducer sensors [14, 16, 7].

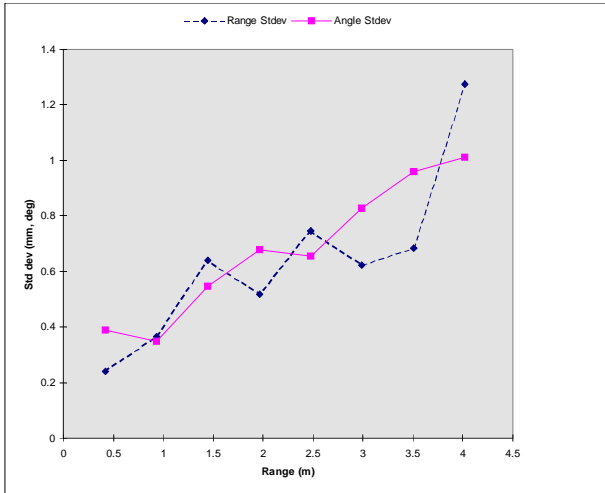


Figure 6 - Standard deviation of range and bearing against range for a plane.

7. Door Finding and Traversal

To illustrate the utility of the scanned sonar sensor, the high level robot task of finding and traversing doorways is chosen. This task is considered difficult by other researchers employing a sonar ring [4] and so is an ideal demonstration for the improved sonar system. A new mobile robot platform developed for sonar sensing mapping and localisation applications is deployed for the task and is shown in Figure 7. The robot has a novel odometry system that uses independent wheels attached to optical shaft encoders and mounted on vertical linear bearings. The odometry wheels carry only their own weight and separate aligned drive wheels provide locomotion. This significantly reduces odometry errors as reported in [5] since drive wheel slippage is decoupled from odometry measurement. The odometry wheels are designed to present a narrow edge to the floor to reduce wheel base uncertainty. The scanned sonar sensor uses the centre transducer in the array mounted on the pan-tilt mechanism on top of the robot. This transducer is placed in the centre of the circular robot. Other features of the robot include a direction bump skirt with 8 micro-switches and motor stall detection since the actual motion of the

robot is monitored not the angular position of the drive wheels as in conventional mobile robots. The software control of the robot is performed with a real-time multitasking operating system.

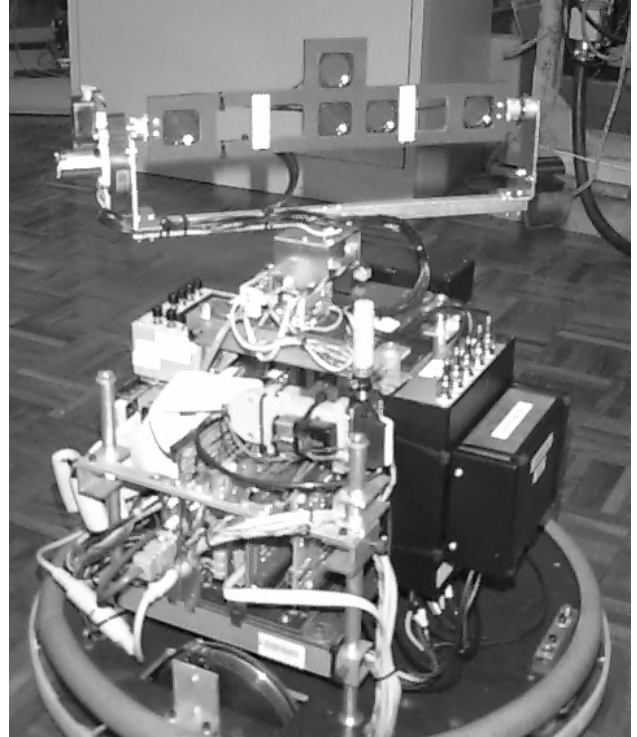


Figure 7 - Robot employed in doorway experiments

The doorway finding and traversal algorithm is performed with a wall following algorithm as follows. After a sonar scan, new targets are added to a list of targets, called the map with the aid of the odometry position and orientation. The nearest target is found from the map, and then the nearest target that is at least 90 degrees away from that target is found - these two targets are denoted by *nearest* and *nearest opposite* targets, as illustrated in Figure 8. Of these two targets the one on the right is used in wall following provided the two targets are at least the robot width plus a safety margin apart. Should the targets be too close together, the nearest target is employed in wall following. Should the nearest and opposite targets be approximately 180 degrees apart and within a range of acceptable doorway sizes, the robot declares that has found a doorway. The robot moves a set distance and scans again.

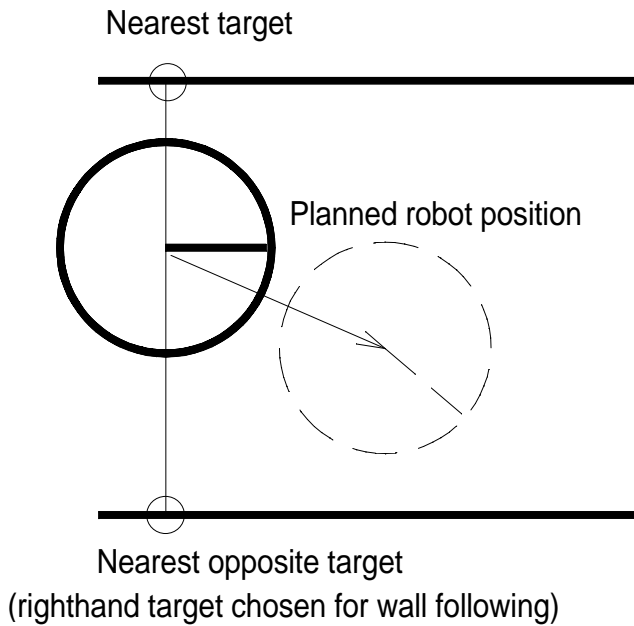


Figure 8 - Wall following.

The wall following algorithm involves moving to a point along the wall a set distance from projected wall position, or if the angle to the new wall target is significantly behind the last wall target the robot turns about the new wall target as shown in Figure 9. In this way convex corners are successfully tracked and in particular narrow doorways are entered even when approached perpendicular to the direction necessary to enter the doorway. If the sonar fails to detect an obstacle, bump sensors and stall detection provide another layer of sensing. When the robot encounters a bump, it turns and heads perpendicular to the detected direction of the bump. Only rarely is the bump sensor activated.

8. Results of Doorway Trials

The doorway finding and traversal algorithm was tested against 6 different “styles” of doorways multiple times. In all cases the robot found the doorway and successfully entered it. Examples of different scenarios are shown in Figures 10, 11 and 12, where the nearest and opposite nearest sonar targets are displayed from each robot position. Thick grey lines have been added to the maps to indicate the actual position of planes in the environment that have been sensed by the sonar.

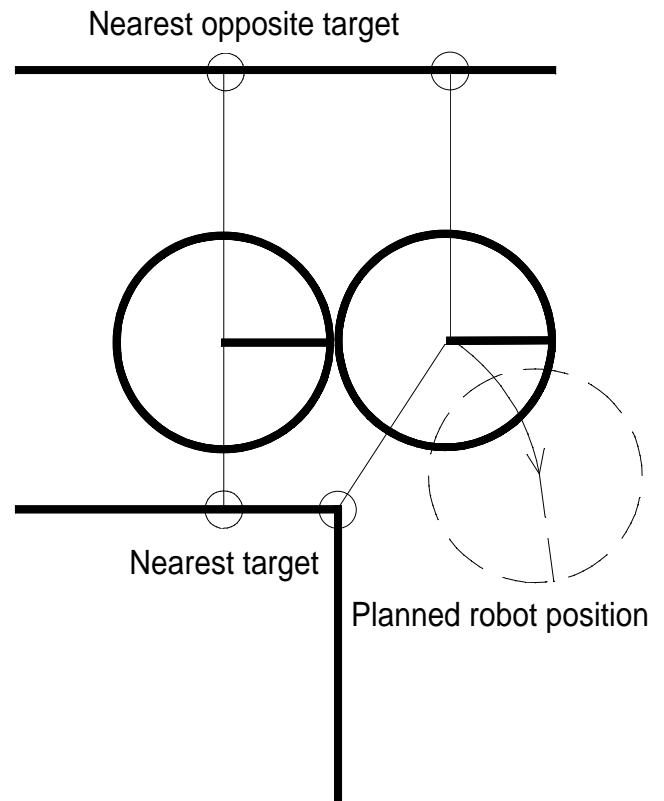


Figure 9 - Wall following - when the righthand target falls behind the previous target the robot performs an arc movement.

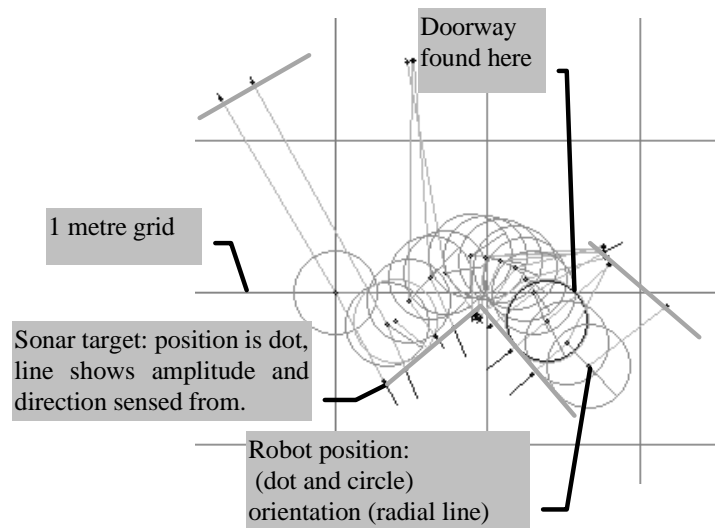


Figure 10 - Experimental results of robot finding and traversing an office doorway from a corridor.

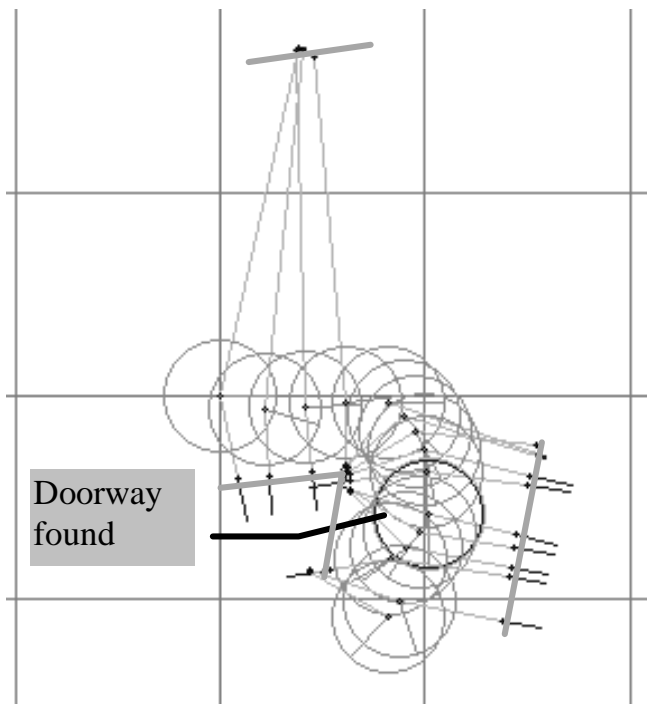


Figure 11 - Another doorway experiment.

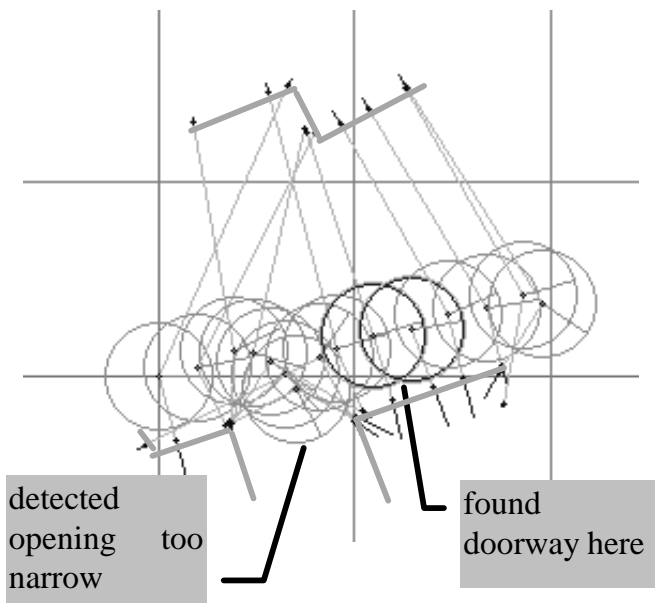


Figure 12 - Robot attempts to initially enter narrow opening but decides against it and enters doorway later.

9. Conclusions and Extensions

A new approach to scanned ultrasonic sensing has been presented that is simple, fast and accurate. With the current hardware approximately 14 scan angles can be processed per second on a 486 ISA bus computer on the robot - the major limitation is the ISA bus throughput. Future hardware employing a PCI bus system should provide optimal speed performance - that is, fire a new pulse as soon as the current receiver period ends. The design is amenable to lower sample rates on a hardware extracted envelope of the echo.

The sensor has been effectively demonstrated in a traditionally challenging environment for sonar systems - finding and traversing narrow doorways. The importance of appropriate low level sensor data processing has been highlighted in this case whereby the high level control of the robot becomes a straight forward matter with reliable low level sensor data.

The approach is being adapted to "on-the-fly" sensing so that the robot need not stop to perform a sonar scan. Other improvements are to focus attention of the sensor on environmental features for faster response to obstacles and changing scenery. Also the scanned monocular approach is aimed to provide fast "scouting" functions for classification sensing [8].

10. Acknowledgments

The help of Greg Curmi is gratefully acknowledged in the detailed design work and construction of the mobile robot. The Australian Research Council large and small grant schemes funded research presented in this paper.

11. References

- [1] O. Bozma and R. Kuc, "Characterizing pulses reflected from rough surfaces using ultrasound," *The Journal of the Acoustical Society of America*, vol. 89, pp. 2519-2531, 1991.
- [2] O. Bozma and R. Kuc, "Characterizing the environment using echo energy, duration, and range: the ENDURA method," presented at IEEE/RSJ International Conference on Intelligent Robots and Systems, Raleigh, NC, 1992 pp. 813-820.
- [3] O. Bozma and R. Kuc, "Building a sonar map in a specular environment using a single mobile sensor," *IEEE Transactions on Pattern Analysis and Machine Intelligence*, vol. 13, pp. 1260-1269, 1991.
- [4] J. Budenske and M. Gini, "Why is it so difficult for a robot to pass through a doorway using ultrasonic sensors?," presented at IEEE Conference on Robotics and Automation, San Diego CA, 1994 pp. 3124-3129.

- [5] K S Chong and L Kleeman, "Precise odometry and statistical error modelling for a mobile robot", Technical report MECSE-96-6, Department of Electrical and Computer Systems Engg., Monash University 1996.
- [6] A Elfes, "Sonar-based real-world mapping and navigation", *IEEE Transaction on Robotics and Automation*, 1987. 3(3): p. 249-265.
- [7] M.L.Hong and L. Kleeman, "A low sample rate 3D sonar sensor for mobile robots", IEEE International Conference on Robotics and Automation 1995, Nagoya, Japan, May 1995 pp. 3015-3020.
- [8] L. Kleeman and R. Kuc, "Mobile robot sonar for target localization and classification," *International Journal of Robotics Research*, Volume 14, Number 4, August 1995, pp 295-318.
- [9] L. Kleeman and R. Kuc, "An optimal sonar array for target localization and classification," presented at IEEE International Conference on Robotics and Automation, San Diego USA, 1994 May pp. 3130-3135.
- [10] R. Kuc, "A spatial sampling criterion for sonar obstacle detection," *IEEE Transactions on Pattern Analysis and Machine Intelligence*, vol. 12, pp. 686-690, 1990.
- [11] R. Kuc and V. B. Viard, "A physically based navigation strategy for sonar-guided vehicles," *International Journal of Robotics Research*, vol. 10, pp. 75-85, 1991.
- [12] J. J. Leonard and H. F. Durrant-Whyte, *Directed Sonar Sensing for Mobile Robot Navigation*: Kluwer Academic Publishers, 1992.
- [13] P. McKerrow, "Echolocation - from range to outline segments," University of Wollongong Preprint no 92/7, November 1992 1992.
- [14] Y. Nagashima and S. I. Yuta, "Ultrasonic sensing for a mobile robot to recognize an environment - measuring the normal direction of walls," presented at IEEE/RSJ International Conference on Intelligent Robots and Systems, Raleigh NC USA, 1992 pp. 805-812.
- [15] A. Ohya, Y. Nagashima, and S. i. Yuta, "Exploring unknown environment and map construction using ultrasonic sensing of normal direction of walls," presented at IEEE International Conference on Robotics and Automation, San Diego, USA, 1994 pp. 485-492.
- [16] H. Peremans, K. Audenaert, and J. M. V. Camperhout, "A high-resolution sensor based on tri-aural perception," *IEEE Transactions on Robotics and Automation*, vol. 9, pp. 36-48, 1993.